2022-02-14

Performance analysis of a runner for gravitational water vortex power plant

Faraji, Adam

Wiley & Sons Ltd

Received: 9 September 2021 | Revised: 19 January 2022 | Accepted: 24 January 2022

DOI: 10.1002/ese3.1085

Energy Science & Engineering
Open Access

MODELING AND ANALYSIS

Performance analysis of a runner for gravitational water vortex power plant

Adam Faraji[1,2] | **Yusufu Abeid Chande Jande**[1,3] | **Thomas Kivevele**[1,3]

[1]Materials and Energy Science and Engineering Department, The Nelson Mandela African Institution of Science and Technology, Arusha, Tanzania

[2]Department of Mechanical Engineering, Arusha Technical College, Arusha, Tanzania

[3]Water Infrastructure and Sustainable Energy Futures centre, The Nelson Mandela African Institution of Science and Technology, Arusha, Tanzania

Correspondence
Adam Faraji, Materials and Energy Science and Engineering Department, The Nelson Mandela African Institution of Science and Technology, Nelson Mandela Rd, P.O. BOX 447, Arusha, Tanzania.
Email: farajia@nm-aist.ac.tz

Abstract

Micro-hydropower can be used to meet the needs of both isolated and rural communities for electricity. Due to its inexpensive initial investment, simple design, easy maintenance and low-head utilisation, the gravitational water vortex power plant (GWVPP) has recently piqued interest. The findings of numerical work employing a numerical simulation and analytical approach for the GWVPP are presented in this study. To understand the influence of each on the efficiency of GWVPP, four parameters (speed, hub-blade angle, number of blades and runner profile) were explored. Design-Expert software was used to investigate the interplay of each parameter/factor in order to maximise the contribution of each. Design-Optimal Expert's (custom) design tool was used to construct twenty-four experimental runs. To calculate the system efficiency, these runs were simulated in commercial computational fluid dynamics (CFD) software called Ansys CFX.

The numerical results were in good agreement with the experimental results, which yielded R^2 values of 0.9507 and 0.9603 for flat and curved profiles, respectively. Furthermore, the findings show that the chosen parameters have an impact on the GWVPP's efficiency via interaction as seen in response surface methodology (RSM). Furthermore, numerical analysis increased the curved blade profile runner's total efficiency by 3.65%. In comparison with the unoptimised scenarios, the efficiency of the flat runner profile increased by 1.69%.

KEYWORDS

blade profile, CFD, gravitation water vortex, micro-hydropower, runner

1 | INTRODUCTION

The enormous dependency on conventional energy resources such as fossil fuel has triggered world concern about environmental awareness, hence has promoted renewable energy resources. Hydropower has proven to be mainly exploited as one of the renewable energy resources due to its wide availability and greater capacity than other renewable sources.[1] However, for the best utilisation of these systems, maintaining the power and frequency stability of the power system plays an important role. Through a hydro-turbine nonlinearity approach, a stability analysis has been performed where results are helpful for practical applications.[2,3] Also, employing mathematical modelling

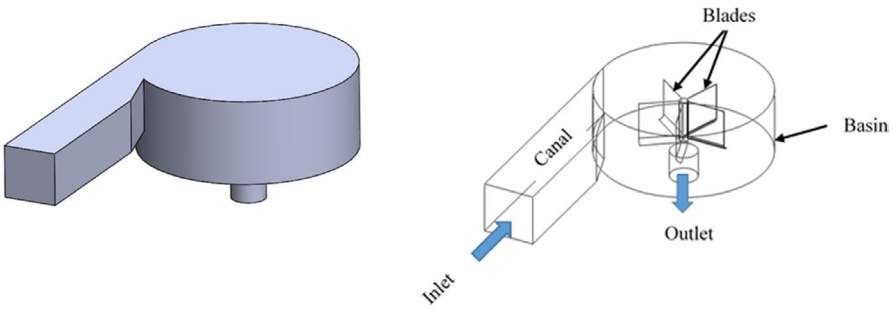

FIGURE 1 Three Dimension (3-D) base case

analysis, stability and damping is studied for large hydropower units.[4,5]

Furthermore, hydropower can be categorised into many types where one of them is micro-hydropower plants. According to Timilsina et al.,[6] micro-hydropower plants are small scale systems that can produce up to 100 kW. This scheme has recently become a growing interest globally because it plays an essential role in power generation in isolated and rural areas.

The gravitational water vortex power plant (GWVPP) is the micro-hydropower scheme applicable mainly in small rivers and streams with low flowrate and low heads. The main three compositions of the GWVPP include a canal, a runner and a basin. GWVPP has been reported to have several advantages such as safe to the environment, ease to manufacture, ease in installation, low costs of operations and maintenance, do not need a reservoir, is safe for aquatic life, increases surface water area, maximises the water velocity of flow on the surface area.[7-9]

Recently, there has been a growing interest in GWVPP. However, there is little work regarding this technology. Researchers have been paying attention to the effect of runner profiles (shapes) on the final performance of the GWVPP. Dhakal et al.[10] numerically studied three runner profiles to determine the most suitable shape. The curved runner profile was reported to have a higher efficiency of 82% than twisted and straight blades, which exhibited 63% and 46% efficiency, respectively. Kueh et al.[11] also experimentally studied the two profiles of the runner. Although the curved profile runner showed better efficiency of 22.24% over the flat profile, which exhibited 21.63%, this study's optimal efficiency was not reached because of the experimental limitations.[11] Khan et al.[8] studied basin to blade ratio configurations by utilising different runner profiles, where the findings revealed that cross-flow blades showing the best efficiency.

The experimental study made by Kueh et al.[11] faced various challenges that could not be solved due to testing limitations. For instance, optimal operating speed was not reached due to practical constraints, failing to determine maximum efficiency. Also, the optimisation of the runner model through various design parameters was not taken into account.

Computational fluid dynamics (CFD) has become a helpful tool for predicting flow patterns and other vital parameters at different conditions. This tool can be utilised during the design process to optimise the design before the actual manufacturing.

The concerns have encouraged the authors to research the use of numerical analysis to overcome experimental limitations at similar conditions to the base case. The same approach will be used to investigate and optimise the GWVPP runner's behaviour by varying speed, hub-blade angle and number of blades. The study aimed to perform numerical analysis and comparative analysis against experimental results for validation purposes. The criteria for evaluation of GWVPP are its final efficiency at different flow conditions under two-phase conditions.

2 | MATERIALS AND METHODS

During this study, numerical methods are used to analyse the efficiency of the GWVPP for flat and curved runner profiles. The base model used in the numerical analysis was chosen from the experimental setup by Kueh et al.[11] The base model was numerically optimised to improve its efficiency. Two phases (air and water at 25°C) were run in Ansys CFX 17.0 at the steady-state with the shear stress transport (SST) turbulence model.

2.1 | Model development

Solidworks software v.2016 was used to create the models. The meshing was done using Ansys ICEM once the established models from Solidworks were transferred. Furthermore, the Ansys ICEM meshed model was imported into the Ansys standalone CFX software, which was used to analyse and optimise the system using the set parameters. The numerical analysis proceeded in the order listed below. To begin, a numerical technique was used to check the agreement of experimental results (for both flat and curved profiles). The optimisation technique was then used, in which selected parameters were changed.

2.2 | Numerical analysis

Solidworks 2016 was used to create three-dimensional (3D) models of the components (canal, runner blades and basin) using the given base design. Four blades with a rotational speed of 4.08 to 2.5 rad/s were confined within a 1000 mm outer runner diameter. The GWVPP model is shown in Figure 1. The guide, which directs the water flow towards the basin, is part of the canal's entrance segment. The runner's rotational velocity is created by the water entering the basin tangentially, and the water is then released axially through the exit.

The computational domains are divided into two parts: a stationary domain that includes the inlet, canal, runner-basin interface, opening, wall and outlet. The rotating domain is the second domain, and it consists of a runner and a runner-basin interface.

Using Ansys ICEM CFD, unstructured tetrahedral mesh computational grids were created on both the stationary and rotational domains. In the Ansys CFX, the stationary and rotating meshes were independently meshed, and then all meshes were connected to a single computational domain. There were a total of 4,380,000 nodes in the network. Figures 2 and 3 illustrate the numerical mesh of the stationary domain (canal and basin) and the rotating domain (runner). The quality of the generated meshes was checked and confirmed using the Ansys ICEM tool.

A total of 4,380,000 nodes were used in this research. This figure was arrived at after a series of tests with meshes ranging from 500,000 to 5,000,000 nodes. The node variation ensures that the final results are not harmed by the amount of nodes.[12] Figure 4 depicts the results of the mesh dependency test. As a result of looking at Figure 4, mesh dependence sensitivity analysis was required. A universal grid interface method was used to create mesh connections between domains and interfaces. The turbulence was predicted using the SST turbulence model. During the numerical study, a two-phase flow with air and water was also used and separated by a discrete interface. Between the basin and runner interface, the frozen rotor was used as a numerical treatment. The set model results yield a steady-state solution for multiple frames of reference.

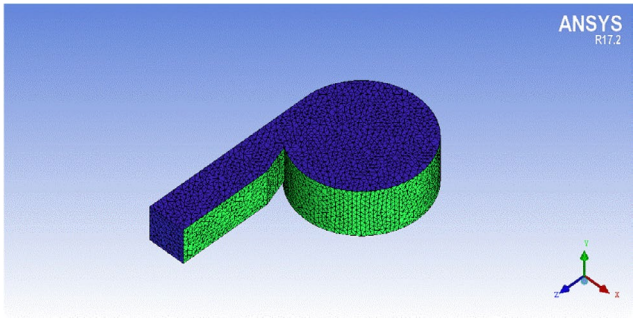

FIGURE 2 Numerical mesh in a stationary domain

The root mean squared (RMS) convergence criteria were utilised, with an average residual target of 1×10^{-4} for mass, momentum and turbulence equations. To achieve adequate convergence, a physical time-step of 0.01 s was used with a maximum iteration of 1000. Figure 5 also shows the mass flow rate of the input portion and the static pressure at the stationary domain output. Tables 1 and 2 provide the design parameters and numerical boundary conditions, respectively.

2.3 | Procedure

2.3.1 | Base model validation

The numerical analysis used the base runner, which was built based on Kueh's experimental work.[11] The parameters of the numerical analysis were retrieved and listed, and their efficiencies were estimated using the parameters of the base model. In each case, the flow pattern and velocity vectors were observed. Ansys CFX was used to assess the base model's agreement with numerical analysis results in the first approach to numerical analysis. There were a total of twenty-four (24) cases run, with the results being recorded.

2.3.2 | Experimental design (selection of optimal parameters)

The effect variables on the efficiency of the GWVPP were investigated using response surface methodology (RSM). RSM is a statistical, scientific and mathematical technique for optimising independent variables while developing models.[13] This feature is available in the Design-Expert software. The RSM approach is a good choice for fitting quadratic surfaces and optimising process inputs with a small number of experiments, as well as analysing parameter interactions. It is a general-purpose strategy that combines design of experiments, regression analysis and optimisation methods to optimise the answers (output variables) that are influenced by numerous independent variables (input variables). Factors used by in RSM include runner speed (A), hub-blade angle (B), blade number (C) and blade profile (D) (D). Table 3 shows how RSM is designed, as well as coded and uncoded levels. This experiment was created using an optimal (custom) design and a quadratic model. A total of twenty-four runs were performed at random, with five interior points, eleven vertex points, six plane points and two edge points.

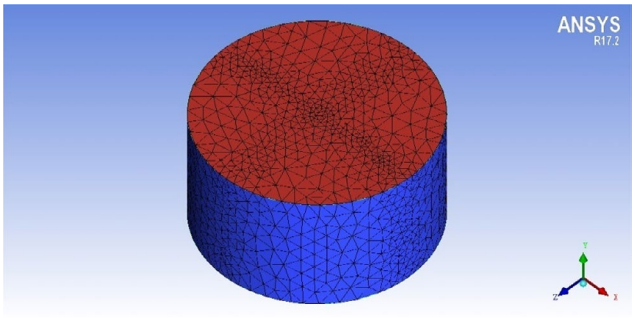

FIGURE 3 Numerical mesh in a rotating domain

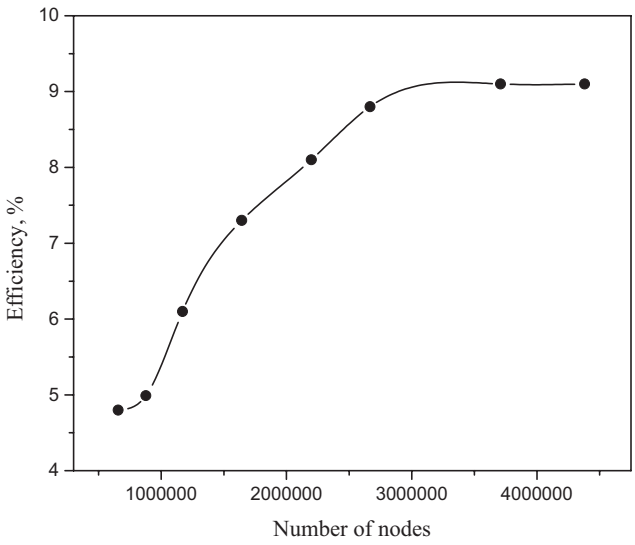

FIGURE 4 Mesh sensitivity analysis

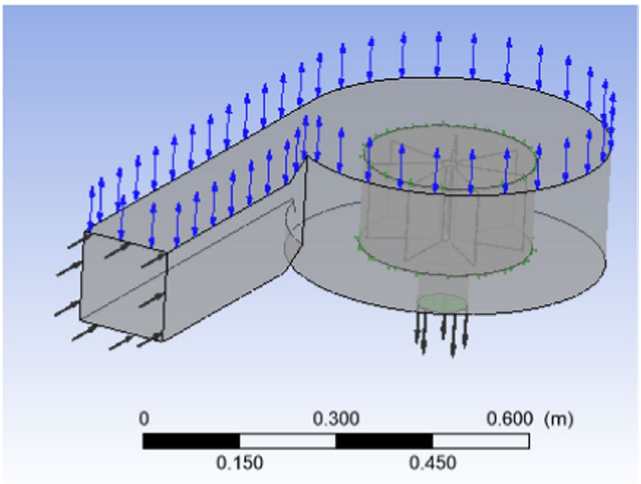

FIGURE 5 Base case setup

2.3.3 | Theoretical performance optimisation of the system

The numerical analysis was utilised to perform analyses that the brake system (in the experimental investigation) was unable to give due to a substantial friction torque needed throughout the experiment. The number of blades tested ranged from 3 to 12, the hub-blade angle varied from 15° to 22° at 1° intervals, and the runner rotational speed varied from 2.62 to 4.08 rad/s. This method aimed to determine the impact of these variables on the GWVPP's overall efficiency. Design-Expert software v.13 was used to produce the best parameter selection and combination. As a result, the base model's efficiency and the optimised model's final efficiency were linked. Additionally, the water flow pattern was observed using simulation techniques such as streamlines.

TABLE 1 Design parameters[11]

Head (H)	0.5 m
Number of blades	3 to 12
Hub-blade angle	15° to 22°
Rotational speed	Varying (2.5 to 4.08 rad/s)
Flow rate (Q)	0.00225 m^3/s
Static pressure	0 Pa

TABLE 2 Numerical boundary conditions

Inlet	Mass flow rate
Outlet	Static pressure (0)
Turbulence model	Shear Stress Transport (SST)
Type of simulation	Steady-state
Phase type	Phase (Air and Water at 25°C)

2.4 | Theory

The Ansys CFX solver can solve the steady-state and transient equations. Mass and momentum equations can be stated as displayed in equations (1) and (2)12:

$$\frac{\partial \rho}{\partial t} + \nabla \cdot (\rho \mathrm{U}) = 0 \tag{1}$$

where ρ denotes density while U displays the vector of velocity $U_{x;y;z}$.

$$\frac{\partial (\rho \mathrm{U})}{\partial t} + \nabla (\rho \mathrm{U} \otimes \mathrm{U}) = -\nabla p + \nabla . \tau + S_{\mathrm{M}} \tag{2}$$

where τ denotes stress tensor and $\otimes$ displays dyadic symbol; S_{M} denotes momentum of the external source term while stress tensor τ is related to the strain rate.[12]

$$\tau = \mu(\nabla \mathrm{U}) + \left(\nabla \mathrm{U}^T - \frac{2}{3}\delta \nabla . \mathrm{U}\right) \tag{3}$$

TABLE 3 Independent variables (RSM optimal custom)

Independent variable	Symbol	Factor	Coded low	Coded high
Runner speed (rad/s)	A	Numerical	2.62	4.08
Hub-blade angle	B	Numerical	15°	22°
Number of blades	C	Numerical	3	12
Blade profile	D	Categorical	Flat	Curved

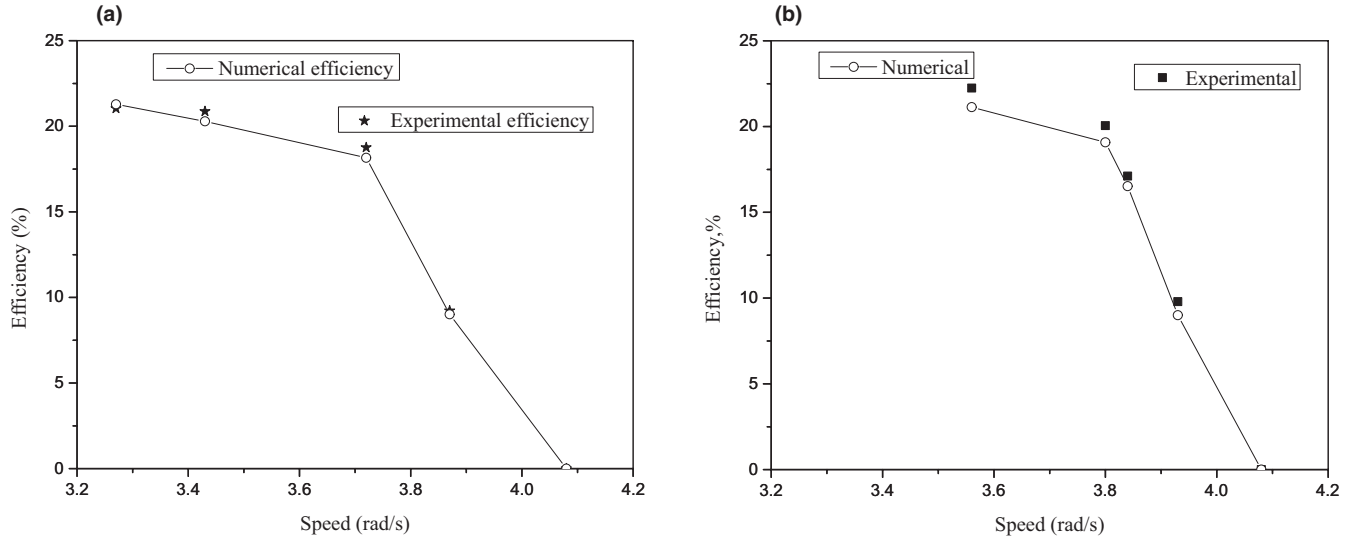

FIGURE 6 Experimental versus numerical (A) flat blade profile (B) curved blade profile

where T denoted static temperature and μ displays molecular viscosity. Mass and momentum conservation equations stated in equation (1) and (2) calculates the velocity fields.

The criteria used to measure the performance of the turbine is its final efficiency. Efficiency is considered as the percentage of the input power to the output power.

2.4.1 | Theoretical Power of the GWVPP

The maximum power output of hydropower can be obtained is as follows[6]:

$$P = \rho g Q H \tag{4}$$

where H is the gross head at the site and Q is the flow rate.

Similar to conventional hydropower, the performance of GWVPP is obtained by using its output efficiency. Because the GWVPP runner is classified as a combination between an impulse and a reaction turbine, the equation is written as Mulligan et al[14]:

$$P_{\text{out}} = T\omega = Q\rho\left(v_{\text{i}} - v_{\text{b}}\right) r\omega \tag{5}$$

where P_{out} is the shaft power of the runner; T is the torque at the shaft while ω is the angular velocity, Q is the flow rate, ρ is water density, v_{i} is the interface velocity between runner and basin, v_{b} is the blade velocity and r is the basin radius.

Interface velocity, runner blade velocity and torque produced were deduced by the available function calculator in the CFD-Post processing. A runner was assigned as a rotating domain. The rotation axis of the runner is selected to be in the y-direction. Angular velocity 'ω' was calculated by using the equation:

$$\omega = \frac{2.N.\pi}{60} \tag{6}$$

Thus, the efficiency of the GWVPP can be calculated by:

$$\eta = \frac{\left(v_{\text{i}} - v_{\text{b}}\right) r\omega}{gH} \tag{7}$$

where v_{i} is the interface velocity, and v_{b} is the blade velocity.

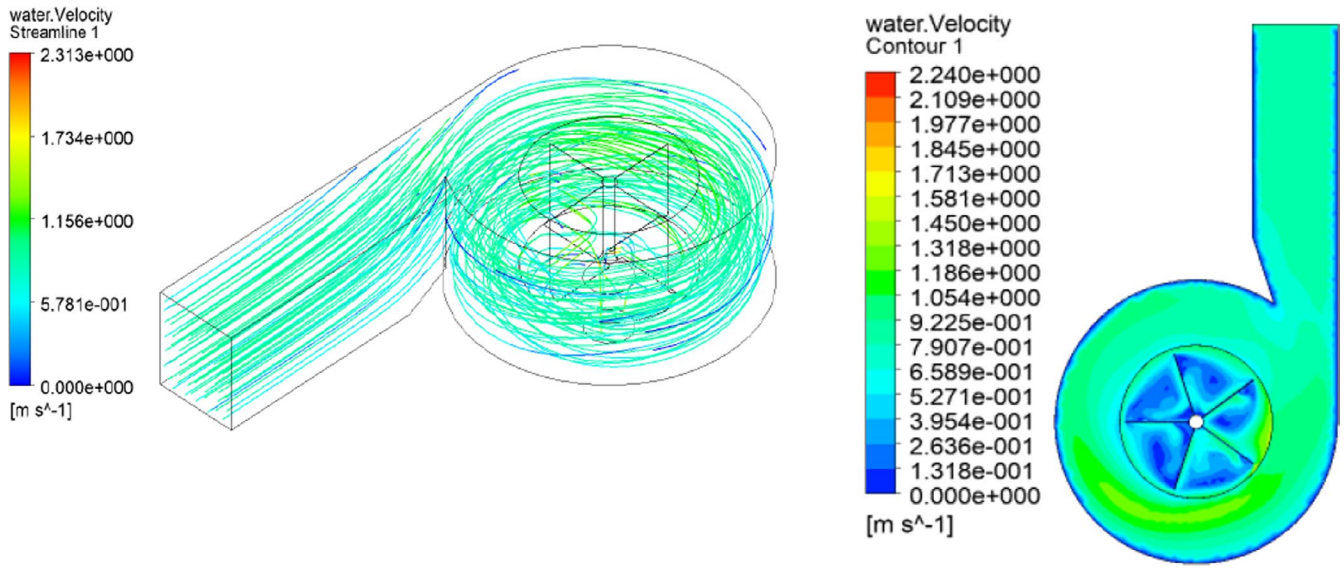

FIGURE 7 Model (A) Streamlines (B) velocity contour

TABLE 4 Simulated factors and their responses

Run	Factor 1 A: speed, rad/s	Factor 2 B: Angle, Degree	Factor 3 C: blades	Response 1 Efficiency (flat), %	Response 2 Efficiency (curved), %
1	3.27664	18	8	16.02	18.07
2	3.6128	18	7	14.08	17.2
3	3.6128	18	7	14.08	17.2
4	2.62	16	6	23.32	25.89
5	4.08	18	12	9.47	11.2
6	3.9048	22	7	10.09	12.88
7	3.32749	15	11	11.28	13.09
8	2.62	17	12	12.05	16.87
9	4.007	18	6	12.48	14.6
10	3.32749	15	11	11.28	13.09
11	4.08	15	12	8.5	9.8
12	3.1821	20	3	15.52	17.3
13	3.6055	22	12	11.82	13.35
14	3.6055	22	12	11.82	13.35
15	3.0799	15	8	17.42	18.2
16	2.8901	15	3	17.55	20.63
17	4.08	22	3	8.08	11.54
18	2.62	22	6	19.32	21.03
19	2.62	20	7	19.89	21.5
20	3.6128	18	7	17.02	18.74
21	4.08	15	3	9.11	12.06
22	3.1821	20	3	15.25	16.9
23	2.839	19	3	18.42	21.24
24	2.62	22	12	13.87	15.55

TABLE 5 Response transformation and model fitting

Response (Efficiency)	Response range	Ratio[a]	Fitting	Transformation
Curved	9.8–25.89	2.64	Quadratic	None
Flat	8.08–23.32	2.89	Quadratic	None

[a]Ratio of maximum to the minimum response.

TABLE 6 ANOVA for the quadratic model

	Flat profile					Curved profile				
Source	Sum of Squares	df	Mean Square	*F*-value	*p*-value	Sum of square	df	Mean square	*F*-value	*p*-value
Model	316.54	9	35.17	30.02	<0.0001	348.20	9	38.69	37.62	<0.0001
A-speed	161.28	1	161.28	137.65	<0.0001	178.28	1	178.28	173.37	<0.0001
B-Angle	0.0103	1	0.0103	0.0088	0.9265	1.82	1	1.82	1.77	0.2047
C-blades	27.94	1	27.94	23.85	0.0002	34.59	1	34.59	33.63	<0.0001
AB	0.0658	1	0.0658	0.0562	0.8161	5.38	1	5.38	5.23	0.0382
AC	25.84	1	25.84	22.05	0.0003	13.87	1	13.87	13.49	0.0025
BC	9.29	1	9.29	7.93	0.0137	11.83	1	11.83	11.51	0.0044
A^2	0.0305	1	0.0305	0.0260	0.8741	3.55	1	3.55	3.45	0.0843
B^2	2.84	1	2.84	2.42	0.1421	8.98	1	8.98	8.74	0.0104
C^2	37.18	1	37.18	31.73	<0.0001	31.73	1	31.73	30.86	<0.0001
Residual	16.40	14	1.17			14.40	14	1.03		
Lack of Fit	10.60	9	1.18	1.02	0.5228	12.74	9	1.42	4.26	0.0625
Pure Error	5.80	5	1.16			1.66	5	0.3322		
Cor Total	332.94	23				362.59	23			

3 | RESULTS AND DISCUSSIONS

3.1 | Validation results

Numerical analysis performed based on the data from the experimental test has shown good agreement with the experimental results. The combined numerical and experimental results for flat and curved tests are displayed in Figure 6. The purpose of these tests was to study the agreement of the numerical approach against the experimental method. For both flat and curved blade profiles, the numerical and experimental results are in good agreement. This result suggests that the numerical approach can further investigate the vortex system for the optimisation process. Figure 7 depicts the streamlines and velocity contours in the internal flow field of GWVPP. From both presentations, some distortion can be observed to due to availability of blades. Some turbulences can also be observed as the result of interaction between runner and the basin.

3.2 | Optimisation of parameters by RSM

The actual design parameters as proposed by Design-Expert software and their corresponding responses as Ansys CFX software are displayed in Table 4. The output presented by Design-Expert software offers an unaliased quadratic model for the efficiency of the GWVPP.

Equations (8) and (9) shows the final models of quadratic equations for GWVPP efficiency.

$$\begin{aligned}\text{Efficiency (flat profile)} = {} & 24.3584 - 7.60184A + 2.11494B - 1.40191C \\ & - 0.0393932AB + 0.588195AC + 0.0671479BC \\ & - 0.171252A^2 - 0.0674256B^2 - 0.142724C^2\end{aligned} \tag{8}$$

$$\begin{aligned}\text{Efficiency (curved profile)} = {} & 56.4381 - 27.5295A + 2.57002B - 1.23527C \\ & + 0.356225AB + 0.430987AC + 0.0757838BC \\ & + 1.84777A^2 - 0.120001B^2 - 0.131851C^2\end{aligned} \tag{9}$$

3.3 | Statistical analysis

3.3.1 | Model fitting

The effects of independent variables, including runner speed (A), hub-blade angle (B), the number of blades (C) and blade profile (D), on the efficiency of the GWVPP are given in Table 5. The results depict that curved blade profile efficiency rose by 3.65% while flat blade improved by 1.69%. In addition, coefficients of the quadratic equation were computed from experimental data to predict the values of the response variable. Observation from Table 6

displays the lack of fit F-value of 1.02 for flat profile, implying the lack of fit is insignificant relative to the pure error. On the other hand, for curved profile, lack of fit, F-value is observed to be 4.26, implying lack of fit is also insignificant.

3.3.2 | Analysis of variance

Analysis of variance (ANOVA) was carried out to ensure proper fit of the derived model. A test for the significance of the regression model and lack of fit coefficient was determined. A confidence level value (*F*-value) and probability value (*p*-value) were employed as a basis for ranking the significant factors. The effectiveness of these factors was ranked in the order of rotational speed > number of blades > hub-blade angle as it can observed in Table 6. ANOVA results in Table 6 indicates outputs of equations (8) and (9). It can be observed from Table 6 that the model of *F*-value of GWVPP efficiency for a flat profile and curved profile are 30.02 and 37.62, respectively, while their corresponding model of *p*-value is less than 0.0001 for both profiles. These *F*-value and *p*-value suggest that the models were significant and statistically accurate, and there is only a 0.01% chance that an *F*-value could occur due to noise. Therefore, the terms A, B, C, AB, AC, BC, A^2, B^2, C^2 are significant model terms.

Table 7 summarises the statistical parameters. This study shows that the R^2 for flat and curved profiles being 0.9507 and 0.9603, respectively, demonstrating that the quadratic model could adequately describe the influence of speed (A), hub-blade angle (B) and blades number (C). Thus, R^2 is closer to one; it indicates a better model fitting to actual data.[13] The predicted R^2 for both responses of flat and curved profiles correlated with adjusted R^2, suggesting the data from Ansys CFX are correct, and their deviations are insignificant. Moreover, these findings indicate that the predicted models for flat and curved profiles can be applied to navigate the design space.

Additionally, the Predicted R^2 of 0.8165 and 0.8555 for flat and curved profiles reasonably agree with the Adjusted R^2 of 0.9191 and 0.9348, respectively; that is the difference is less than 0.2.

The graph of actual versus simulated data was plotted to establish the validity of the model. The residuals show the difference between the experimented data and the predicted value. Figure 8a,b presents the correlation between predicted and simulated data; all data were found around the line of best fit, suggesting that the simulated

TABLE 7 Statistical parameters

Parameter	Flat profile	Curved profile
Standard deviation	1.08	1.01
Mean	13.99	16.30
C.V. %	7.74	6.22
R^2	0.9507	0.9603
Adjusted R^2	0.9191	0.9348
Predicted R^2	0.8165	0.8555
Ade. precision	19.0980	23.0059

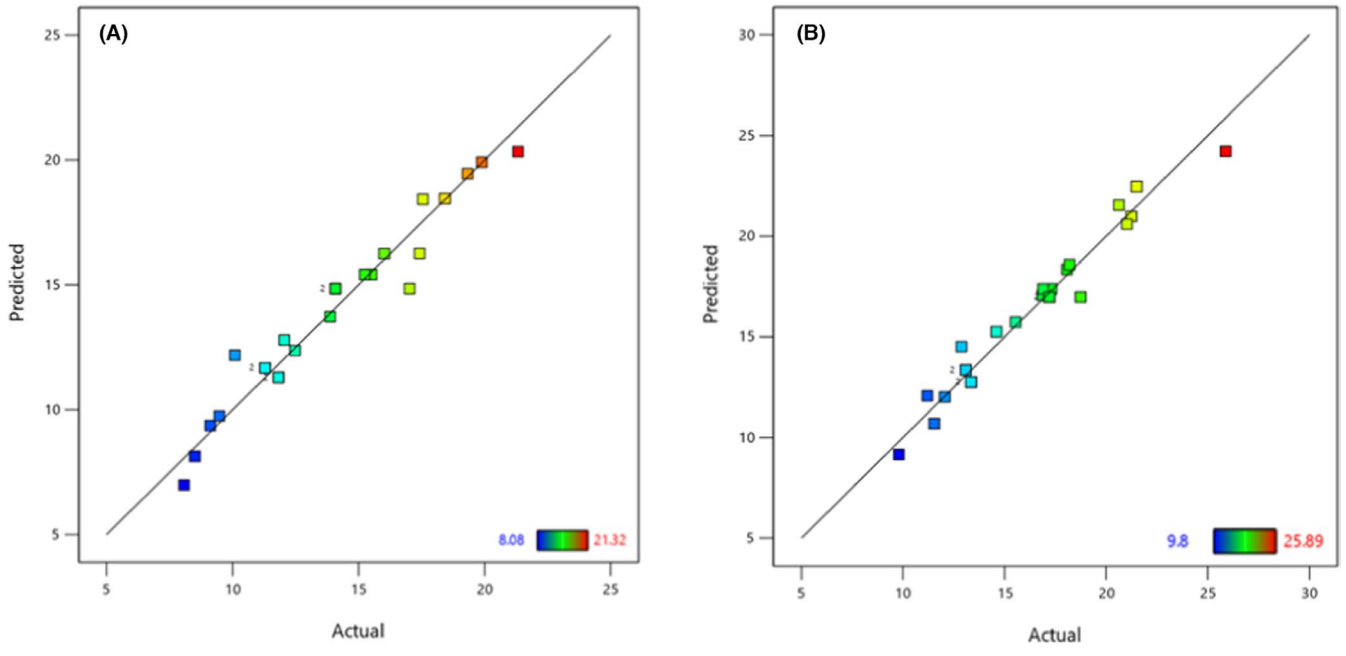

FIGURE 8 Predicted value versus simulated value for the yield of (A) flat profile (B) curved profile

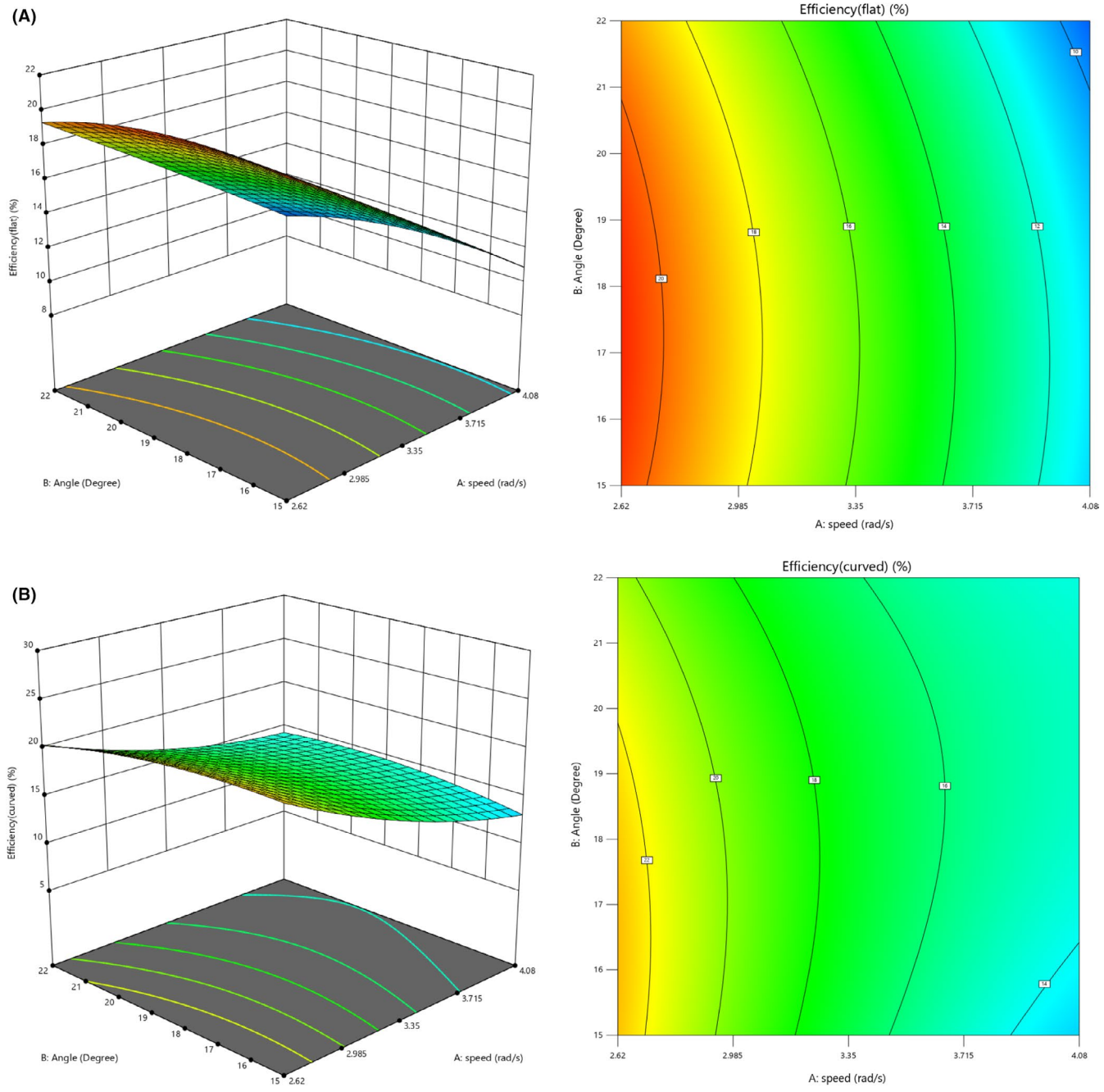

FIGURE 9 3D plot and contour for (A) flat profile and (B) curved profile (factors A and B)

data agreed with predicted values without any abnormalities in the models.

3.4 | Discussion: Derived models interpretation

The Response graphs obtained from the Design-Expert software has provided the best visualisation of interactions for the factors under study. Three dimensional (3D) and contour plots were developed to understand the interactions of each parameter and establish their contribution towards the final efficiency of the GWVPP.[15] The surface plots (3D and contour) for the flat and curved runner profiles are displayed in Figures 9–11. Figure 9 shows the interactions of two factors, namely, factor A (speed) and factor B (hub-blade angle) to check their influence against factor D (blade profiles i.e. flat and curved). The effect of these two factors on the final efficiency of the GWVPP for the flat and curved profiles is observed. The plots reveal that both parameters, speed and hub-blade angle contribute to the efficiency of the GWVPP at a particular range for all profiles under study. For example,

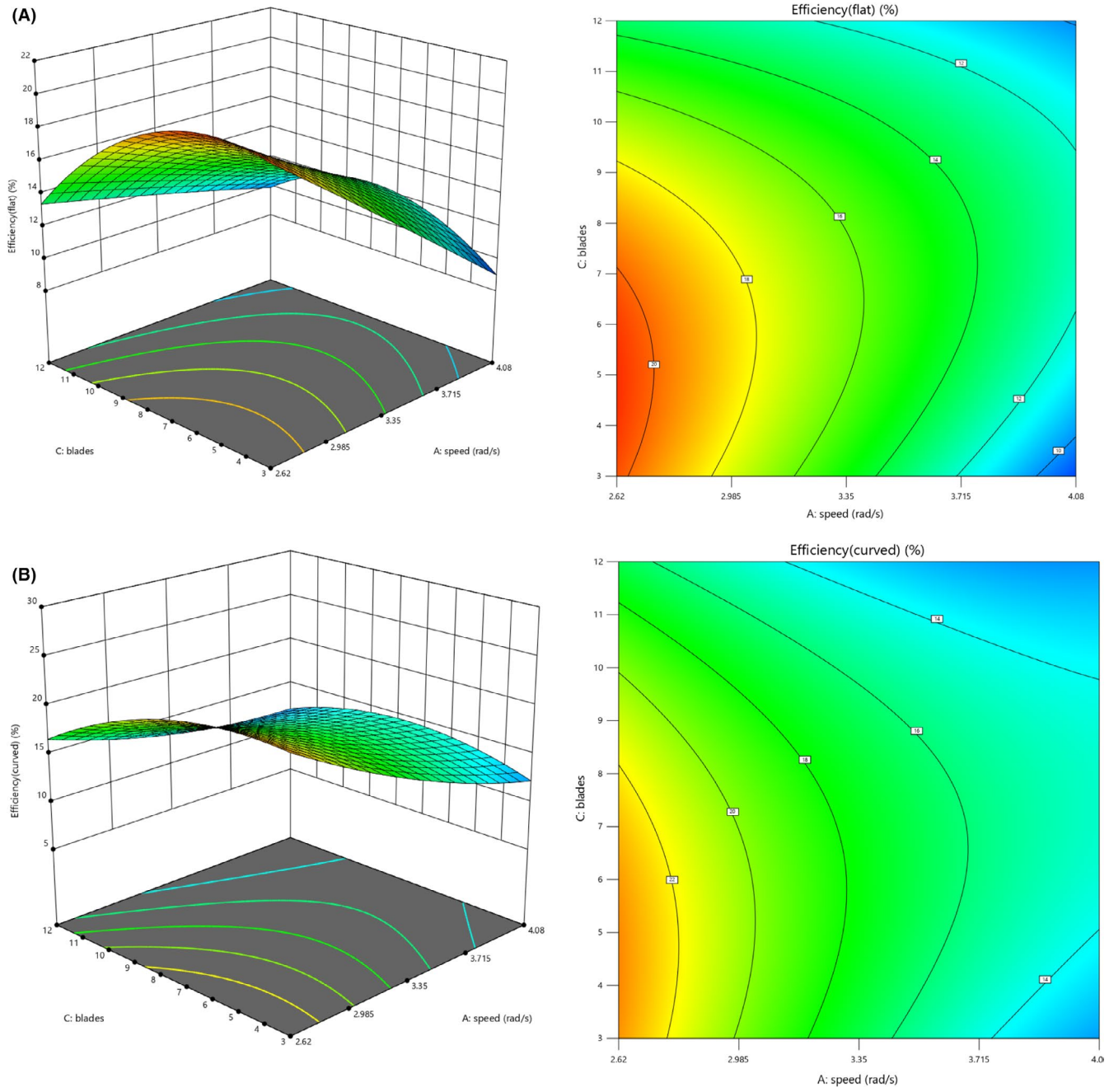

FIGURE 10 3D plot and contour for (A) flat profile and (B) curved profile (factors A and C)

although a shallow bell-shaped structure can be seen in the flat profile in Figure 9A, the strong bell-shaped is observed in curved profiles in Figure 9B. This result suggests that these factors are crucial in the performance of the GWVPP and are in agreement with the works of literature.[6-9]

Also, the effect of interactions of factor A (speed) and factor C (number of blades) to factor D (blade profiles i.e. flat and curved), as displayed in Figure 10, was studied. A clear bell-shaped structure is seen for the flat profile in Figure 10A, while for the curved profile in Figure 10B, the twisting of the plots is observed. Again, these results suggest that these factors are essential in the performance of GWVPP, although the twist seen in the curved profile may mean two factors are not optimally blended.[8]

Moreover, the combination of factor B (hub-blade angle) and factor C (number of blades) to factor D (blade profiles i.e. flat and curved) is considered to observe their effect on the efficiency of the GWVPP.

For both flat, Figure 11A and curved, Figure 11B profiles depict a bell-shaped structure plot. This behaviour suggests that these two factors have a significant contribution to the efficiency of the GWVPP. As per several works of literature,[6-8,10,16] runner speed typically

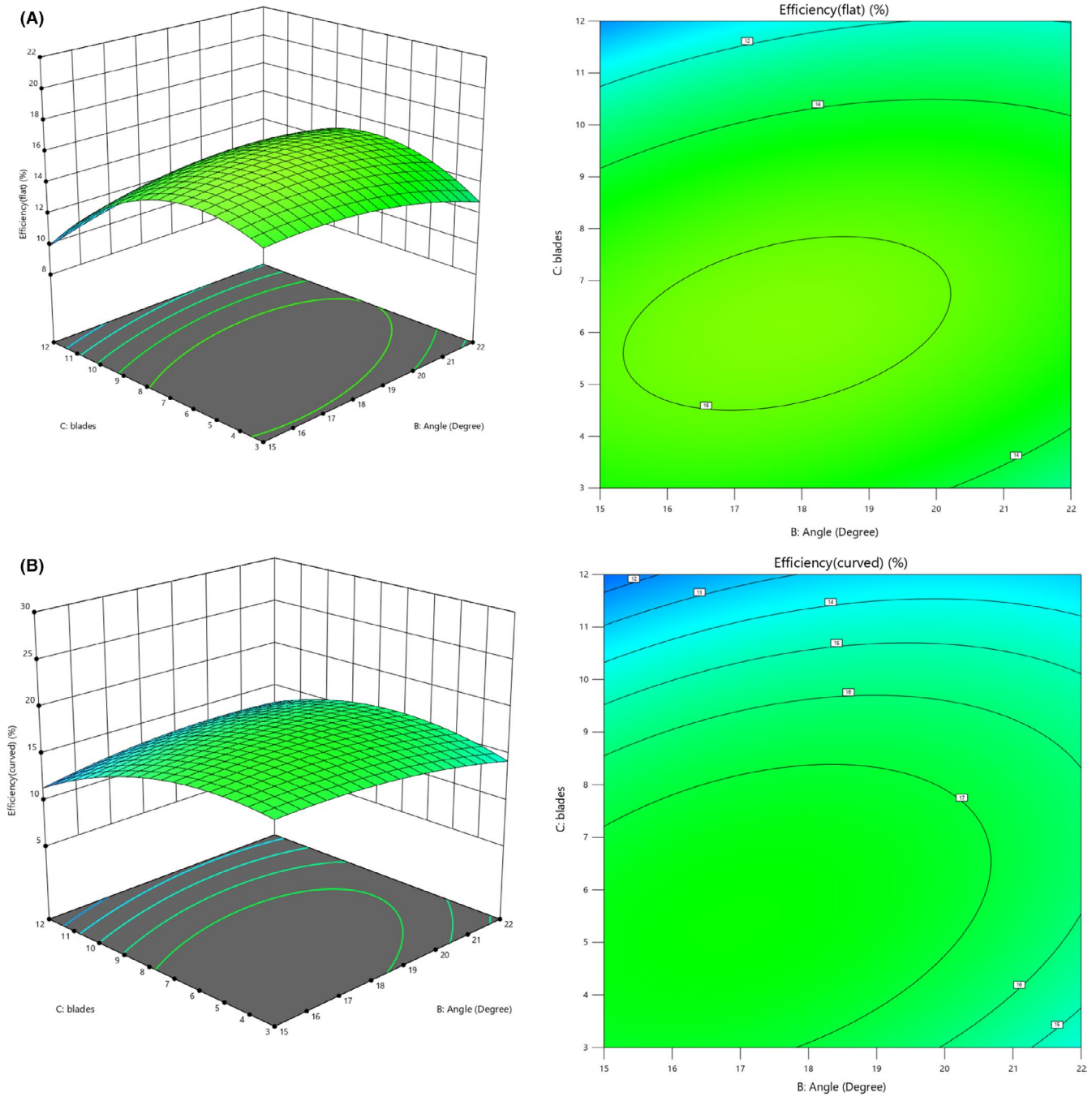

FIGURE 11 3D plot and contour for (A) flat profile and (B) curved profile (factors B and C)

follows the bell-shaped structure implying that the efficiency of the GWVPP increases as speed rises. Still, after reaching a certain speed (optimal), the efficiency starts to fall.

4 | CONCLUSION

The paper examined the application of CFD for the validation of experimental tests. Essential components regarding GWVPP were modelled in 3D by using the Solidworks software. The modelled features include; water canal, the water basin (both considered stationary domains) and the runner (considered rotating domain). On the other hand, Design-Expert through RSM was utilised to optimise the interactions of factors. RSM gave the combination of each parameter to get the optimum blend. The study has further used CFD software to study and predict the effect of four parameters on the efficiency of the GWVPP. These parameters include runner speed (A), hub-blade angle (B), the number of blades (C) and blade profile (D) designed along with coded and

uncoded levels. Through the blending of these four parameters, the system efficiency is improved. The reason being the applied approach minimised one-factor-at-a-time (OFAT) selection limitations. The study shows that a numerical approach together with proper blending of parameters can be used to perform an analysis of the GWVPP. Also, Design-Expert software can be exploited to determine the combinations of parameters. Results of the investigation have shown good agreement with the experimental work. Additionally, the results show that the chosen parameters affect the GWVPP through interaction observed in RSM.

Furthermore, numerical analysis improved the runner's overall efficiency of curved blade profile by 3.65%. In contrast, the efficiency of the flat runner profile rose by 1.69% compared to the unoptimised cases. The observed results depict that it is possible to validate experimental results using Ansys CFX as one of the CFD tools.

ACKNOWLEDGEMENTS

The authors acknowledge the following: (i) the Water Infrastructure and Sustainable Energy (WISE Futures) centre under the Nelson Mandela African Institution of Science and Technology (NM AIST) for their financial support and (ii) the PIV lab of Korea Maritime and Ocean University (KMOU) for valuable support during Ansys CFX analysis.

ORCID

Adam Faraji https://orcid.org/0000-0001-8627-7729
Thomas Kivevele https://orcid.org/0000-0003-4539-6021

REFERENCES

1. Okot DK. Review of small hydropower technology. *Renew Sustain Energy Rev*. 2013;26:515-520.
2. Liu D, Li C, Malik O. Nonlinear modeling and multi-scale damping characteristics of hydro-turbine regulation systems under complex variable hydraulic and electrical network structures. *Appl Energy*. 2021;293:116949.
3. Liu D, Wang X, Peng Y, et al. Stability analysis of hydropower units under full operating conditions considering turbine nonlinearity. *Renew Energy*. 2020;154:723-742.
4. Liu D, Li C, Malik OP. Operational characteristics and parameter sensitivity analysis of hydropower unit damping under ultra-low frequency oscillations. *Int J Electr Power Energy Syst*. 2022;136:107689.
5. Liu D, Li C, Tan X, Xueding L, Malik O. Damping characteristics analysis of hydropower units under full operating conditions and control parameters: accurate quantitative evaluation based on refined models. *Appl Energy*. 2021;292:116881.
6. Timilsina AB, Mulligan S, Bajracharya TR. Water vortex hydropower technology: a state-of-the-art review of developmental trends. *Clean Technol Environ Policy*. 2018;20:1737-1760.
7. Dhakal S, Nakarmi S, Pun P, Thapa AB, Bajracharya TR. Development and testing of runner and conical basin for gravitational water vortex power plant. *J Inst Eng*. 2014;10:140-148.
8. Khan NH, Cheema TA, Chattha JA, Park CW. Effective Basin–Blade configurations of a gravitational water vortex turbine for microhydropower generation. *J Energy Eng*. 2018;144:04018042.
9. Rahman MM, Tan JH, Fadzlita MT, Muzammil ARWK. A review on the development of gravitational water vortex power plant as alternative renewable energy resources. In: *International Conference on Materials Technology and Energy*. IOP Publishing; 2017;217:012007.
10. Dhakal R, Bajracharya TR, Shakya SR, et al. Computational and experimental investigation of runner for gravitational water vortex power plant. In: *2017 IEEE 6th International Conference on Renewable Energy Research and Applications (ICRERA)*. IEEE Publisher; 2017:365-373.
11. Kueh TC, Beh SL, Ooi YS, Rilling DG. Experimental study to the influences of rotational speed and blade shape on water vortex turbine performance. In: *Fifteenth Asian congress of fluid mechanics (15ACFM)*. IOP Publishing; 2017;822:012066.
12. CFX Ansys. Ansys Cfx-solver theory guide. *ANSYS CFX Release*. 2009;15317:724-746.
13. Montgomery DC, Myers RH, Anderson-Cook CM. *Response Surface Methodology – Process and Product Optimization Using Designed Experiments*. WILEY; 2016.
14. Mulligan S, Casserly J. *The Hydraulic Design and Optimisation of a Free Water Vortex for the Purpose of Power Extraction*. Institute of Technology Sligo; 2010.
15. Wanchat S, Suntivarakorn R, Wanchat S, Tonmit K, Kayanyiem P. A parametric study of a gravitation vortex power plant. *Adv Mater Res*. 2013;805-806:811-817.
16. Power C, McNabola A, Coughlan P. A parametric experimental investigation of the operating conditions of gravitational vortex hydropower (Gvhp). *J Clean Energy Technol*. 2016;4:112-119.

How to cite this article: Faraji A, Jande YAC, Kivevele T. Performance analysis of a runner for gravitational water vortex power plant. *Energy Sci Eng*. 2022;00:1–12. doi:10.1002/ese3.1085